Environmental Science and Pollution Research (2021) 28:34697–34713
https://doi.org/10.1007/s11356-021-13132-0

RESEARCH ARTICLE

Effects of zinc oxide nanoparticles on antioxidants, chlorophyll contents, and proline in *Persicaria hydropiper* L. and its potential for Pb phytoremediation

Fazal Hussain[1] · Fazal Hadi[1,2] · Qiu Rongliang[2]

Received: 10 August 2020 / Accepted: 19 February 2021 / Published online: 3 March 2021

Abstract

Applications of nanoparticles and plants for efficient restoration of heavy metal-polluted water and soil are an emerging approach and need to be explored. Hydroponic study was performed to find the role of zinc oxide nanoparticles (ZnO NPs) in plant growth, antioxidative response, and lead (Pb) accumulation in *Persicaria hydropiper*. Seedlings were grown in Pb-polluted media amended with 5, 10, 15, and 20 mg L^{-1} ZnO NPs. Inductively coupled plasma spectroscopy (ICP) was used for Pb analysis in plant tissues. Pb significantly inhibited seedling growth, and ZnO NPs alleviated Pb-induced stress by promoting plant growth, and improved chlorophyll and carotenoid contents. Oxidative stress ameliorated in ZnO NPs exposed seedlings through enhanced production of free proline, phenolics, flavonoids, and activation of antioxidative enzymes. Pb accumulation boosted in ZnO NP treatments, and highly significant increase in Pb accumulation in roots (255.60±4.80 mg kg^{-1}), stem (124.07±2.84 mg kg^{-1}), and leaves (92.00±3.22 mg kg^{-1}) was observed in T3 (15 mg L^{-1} ZnO NPs) for *P. hydropiper*. Contrarily, ZnO NPs at 20 mg L^{-1} dose suppressed plant growth, Pb accumulation, secondary metabolites, and antioxidative enzyme activities. Moreover, positive correlation was found in Pb accumulation with free proline and secondary metabolite contents in plant tissues. These results suggest that ZnO NPs at optimum concentration may augment efficacy of plants to remove heavy metal from polluted water through nanophytoremediation.

Keywords ZnO nanoparticles · Pb phytoaccumulation · *Persicaria hydropiper* L · Hydroponic growth · Phenolics · Antioxidant enzymes

Introduction

Due to rapid industrialization, heavy metal pollution has become a global problem and to be addressed seriously (Cox et al. 2016; Duarte et al. 2010). Heavy metal-polluted water and soil have devastating effects on crop growth and productivity and cause huge economic losses (Pant and Tripathi 2014). In some developing countries, most industrial wastes containing toxic metals are directly discharged into agricultural lands and water resources without any proper treatment (Azizullah et al. 2014; Singh et al. 2012). Through food chain, these toxic heavy metals eventually reach human and animal bodies and pose severe threats to their health (Balseiro-Romero et al. 2017). The ruthless manipulation of water resources has caused pollution of water bodies with toxic heavy metals (Ullah et al. 2018).

Lead (Pb) is one of the toxic heavy metals and is lethal even at very low concentrations to both humans as well as plants life without known biological functions (Wang et al. 2018). It pollutes water and soil due to diverse natural and anthropogenic activities (Hadi et al. 2010; Kabir et al. 2009). Pb toxicity causes several highly fatal health complications like neurotoxicity, impaired fertility, anemia, hypertension (Sthanadar et al. 2013), and cancer of multiple organs (Kamaraj et al. 2015; Offor et al. 2017). For environmental sustainability, highly efficient and

Responsible Editor: Elena Maestri

✉ Fazal Hadi
dr.fhadi@uom.edu.pk; fazalbiotech@yahoo.com

[1] Department of Biotechnology, University of Malakand, KP, Chakdara 18800, Pakistan

[2] School of Environmental Science and Engineering, Sun Yat-Sen University, Guangzhou 510275, China

ecofriendly technologies are to be developed to restore metal-contaminated water and soil (Gunathilakae et al. 2018; Hadi et al. 2016). Phytoremediation using green plants provides a feasible solution to overcome water and soil contamination (Cardwell et al. 2002; Hasan et al. 2007). Heavy metal stress adversely affects plant growth and ultimately reduces plant metal–accumulating capacities (Falkowska et al. 2011; Tassi et al. 2008). Plants under metal stress produce reactive oxygen species (ROS) which causes oxidative stress and eventually result in cell death. To cope metal toxicity, plants are equipped with antioxidative defense mechanism comprising of antioxidant enzymes and plant secondary metabolites like phenolics, flavonoids, and proline. These enzymes and antioxidant compounds directly or indirectly protect different cell organelles from the oxidative damage of ROS produced inside the cells. Phenolics, flavonoids, and free proline act as metal chelators, osmoprotectants, free radical scavengers, prevent lipid peroxidation, and thus play role in plant protection and stress tolerance (Ullah et al. 2019).

Nanoparticles (NPs) are considered as materials of new millennium. Metal-based nanomaterials are well studied and widely used (Prasad et al. 2012). Materials having at least one dimension of 100 nm or less are classified as nanoparticles (Preetha and Balakrishnan 2017). They acquire some unique features such as high functionality and high reactivity due to small size and large surface area (Elmer et al. 2018; Raliya et al. 2017). Nanoparticles exhibit both positive as well as harmful influences on growth and development of plants. Yang et al. (2007) reported that TiO_2-NPs enhanced chlorophyll, nitrogen, protein, and biomass in *Spinacia oleracea* L. Similarly,TiO_2-NPs (0.5 g L^{-1}) stimulated growth of *Lemna minor* L. raised on culture media, while at higher levels, plants were adversely affected (Song et al. 2012). Likewise, zinc oxide nanoparticles (ZnO NPs) showed positive impact on *Cicer arietinum* L. and *Vigna radiata* L. under in vitro culture (Mahajan et al. 2011). Similarly, *Cucumis sativus* L. growth was significantly promoted with ZnO NPs at lower concentration; however, its higher dose inhibited growth (Zhao et al. 2013). Since last decade, nanomaterials are widely exploited to remediate metal-polluted soil and water (Jiang et al. 2017; Lai et al. 2016; Tang et al. 2014). Nanoparticles and green plants synergistically dealt various toxic pollutants (Ma and Wang 2010). Graphene oxide nanoparticles enhanced accumulation of cadmium in *Microcystis aeruginosa* Kutzing (Tang et al. 2015). Higher uptake of trinitrotoluene in *Panicum maximum* Jacq. with iron nanoparticles was reported by Jiamjitrpanich et al. (2013). Similarly, nanoscale iron improved phytoaccumulation of polychlorinated biphenyls along with better growth of *Impatiens balsamina* L. and could augment pollutant removal efficiency from soil (Gao and Zhou 2013).

Zinc metal (Zn) is the most important micronutrients needed for optimum growth and development of plants (Saxena et al. 2016). It is required for synthesis of chlorophyll, lipid, protein, and carbohydrates, and acts as cofactor for enzymes and is a pre-requisite for proper hormonal functioning (Hussein and Abou-Baker 2018). Nanostructured formulation of ZnO is widely used as an adsorbent for heavy metal removal from polluted water (Ma et al. 2010; Wang et al. 2010). Due to their high metal adsorption capacity, zinc oxide nanoparticles are used to remediate metal-polluted water and soil (Hua et al. 2012; Salehi et al. 2010). .

Persicaria hydropiper L. a perennial herb (Fig. 1) belongs to family Polygonaceae (Ayaz et al. 2016; Pooja et al. 2018). The species has worldwide distribution and aggressively growing in damp places in Africa, Europe, Australia, and Asia including Pakistan (Huq et al. 2014; Miyazawa and Tamura 2007). It is hyper accumulator of manganese (Yang et al. 2018). Rapid growth, metal tolerance, and unpalatable nature to herbivores make it a potential candidate plant for effective phytoremediation of Pb-polluted water and soil (Chu 2014; Holm et al. 1997).

Present study was executed with objectives to find out the role of ZnO NPs (1) on plant growth, (2) secondary metabolite production, (3) antioxidant enzyme activity, and (4) Pb accumulation (phytoremediation) in *P. hydropiper* plant in hydroponic condition.

Materials and methods

Zinc oxide nanoparticle synthesis

For biosynthesis of zinc oxide nanoparticles (ZnO NPs), fresh leaves of *Sageretia theezans* Brongn. were procured from wild plants in Dir Lower, Khyber Pakhtunkhwa, Pakistan. Then leaves were extensively washed by running tap water and later on four times rinsed with distilled water to eliminate surface bound dust particles. Subsequently, leaves were shade dried and pulverized in powder form through commercial blender. For extract preparation, leaf powder (10 g) was mixed with deionized distilled water (100 mL) and properly dissolved by stirring for 1 h (80 °C) using magnetic hotplate.

Fig. 1 *Persicaria hydropiper* L.

To get clear filtrates, the resulting mixture was three times sifted through Whatman No. 1 filter paper (Aperture size: 8 μm). The filtrate obtained was utilized as potential source of phytochemicals required for reduction and stabilization of zinc oxide nanoparticles (Thema et al. 2016).

Synthesis of ZnO NPs using leaf extract of *S. theezans* was done by the protocol of Al-Dhabi and Valan (2018) with minor modification. Leaf extract (20 mL) of *S. theezans* was drop wise added to 80 mL of zinc acetate dihydrate (Sigma Aldrich) solution (1mM) under constant stirring at magnetic stirrer hotplate at room temperature. Subsequently, the resulting mixture was retained in water bath for 3 h at 60 °C temperature. The formation of ZnO NPs was confirmed visually and validated by UV-visible spectroscopy. Later on, the solution was centrifuged (10,000 rpm) for 15 min. Then, pellet of the nanoparticles was multiple times washed with ethanol and finally rinsed with deionized water to get pure ZnO NPs. The resultant samples of ZnO NPs were dried in microwave oven at 80 °C for 2 h to evaporate moisture and were used for further characterization.

ZnO nanoparticle characterization

The bio-fabricated ZnO NPs were thoroughly characterized through different spectroscopic and microscopic techniques. Synthesis and stability of ZnO NPs were confirmed via UV-visible spectrophotometer (Shimadzu UV-1800, Japan). Various functional groups attached with ZnO NPs were identified via Fourier transform infrared (FTIR) spectrophotometer (Nicolet iS50 FTIR Spectrometer, USA). FTIR analysis was performed using potassium bromide at transmission mode in frequency range of 400–4000 cm^{-1} at room temperature. The size and crystalline nature of ZnO NPs was determined with X-ray diffraction spectroscopy. The dried samples of ZnO NPs were used to record diffraction patterns via X-ray diffractometer (Shimadzu-Model XRD 6000). The instrument was operated at 40 kV with 30-mA current using Cu/Kα radiations to scan 2θ in range of 10–80°. To estimate average particle size of the nanoparticles, Debye-Scherrer equation was used: $D = k\lambda/\beta\cos\theta$, where D= particle size (nm), k = shape factor (0.94), λ=X-ray wavelength (λ=1.5418 Å), β= full width at half maximum (FWHM), and θ=Bragg's angle. To ascertain, elemental composition and chemical purity of ZnO NP samples, energy dispersive X-ray (EDX) spectroscopic analysis was executed with EDX detector (Oxford Instruments AZTEC EDS) attached to scanning electron microscope (SEM).The morphology and particle size of ZnO NPs were determined through scanning electron microscope (JSM5910 JEOL, Japan). Moreover, hydrodynamic size and zeta potential of the biofabricated ZnO NP suspensions in liquid growth media were investigated with dynamic light scattering (DLS) technique by using Zetasizer Nano-ZS90 (Malvern Instruments, UK).

Seedling collection

Seeds of *P. hydropiper* were collected from Herbarium, University of Malakand, Pakistan. Healthy seeds were selected and allowed to germinate in fertile soil in green house. Two days before sowing seeds, soil (6.82±0.18 pH) was thoroughly watered according to its water holding capacity (350±7.0 mL water kg^{-1} soil). After sowing of seeds, soil was regularly watered after 3-day interval to maintain soil moisture. After germination (15 days), uniform sized seedlings were selected for transplantation in hydroponic experiments.

Growth media and addition of lead

Hoagland's solution (Hoagland and Arnon 1950) was used as growth media throughout the hydroponic culture. Media were prepared as per standard protocol and Pb in the form of lead nitrate [$Pb(NO_3)_2$] was added at 50 mg L^{-1} concentration and mixed. Then media were equally distributed (100 mL per flask) into flasks and were arranged in completely randomized design. For each treatment as well as control, three replicate flasks were used and the whole experimental work was repeated twice.

Seedling transplantation and growth

For transplantation, healthy seedlings were selected and thoroughly washed with tap water and subsequently three times rinsed with sterile distilled water to wash off any dust particles. Then plantlets were transplanted in flasks with growth media (single plantlet per flask). Flasks were properly covered with aluminum foil. Fresh Hoagland's solution of the same composition was regularly supplied to flasks in order to retain constant media volume (100 mL) and to avoid nutrient deficiency during the course of experiments. All plantlets were maintained for 1 month at 25±2 °C in light and dark photoperiods of 16/8 h at approximately 60–70% relative humidity in the growth chamber (BJPX-A1500C, China).

Nanoparticle treatments

Four different concentrations (5, 10, 15, and 20 mg L^{-1}) of ZnO NPs were applied to plantlets after transplantation. Aqueous suspensions of nanoparticles were well dispersed by sonication for 30 min (Toshiba, Japan) before addition to growth media. Plantlets without Pb exposure (C) were compared to Pb-treated plants (C1) in order to assess the impact of Pb stress on plant growth. Similarly, seedlings exposed to Pb only (C1) were compared to ZnO NP-treated seedlings to find influence of different levels of ZnO NPs on plant growth and Pb uptake. Treatments used during hydroponic experiments: C (Control without Pb), C1 (Control with Pb: 50 mg L^{-1}), T1 (50 mg L^{-1} Pb + 5 mg L^{-1} ZnO NPS), T2 (50 mg L^{-1} Pb+

10 mg L^{-1} ZnO NPs), T3 (50 mg L^{-1} Pb+15 mg L^{-1} ZnO NPs), and T4 (50 mg L^{-1} Pb+20 mg L^{-1} ZnO NPs).

Plant harvesting and data collection

After 30 days of treatment application, all treated and control plants were carefully harvested. Then roots were thoroughly washed with deionized water and finally rinsed twice with 5 mM EDTA solution to eradicate surface bound metal ions. Stem and root length were determined by centimeter ruler. Then plants were chopped into leaves, stems, and roots and fresh biomass was recorded with digital balance. Plant tissues were properly packed in labeled small paper envelops and oven dried at 80 °C for 60 h. The dry biomass of various plant organs was separately determined using digital balance. Dried plant samples were crushed into powder form by grinding using mortar and pestle and stored in freezer until further analysis.

Photosynthetic pigment estimation

Chlorophylls (a & b) and carotenoid content in *P. hydropiper* leaves were estimated following procedure of Sumanta et al. (2014). Fresh leaves (0.5 g) were thoroughly homogenized in 80% acetone (10 mL) and centrifuged (10,000 rpm) for 15 min. Supernatants were isolated in clean test tubes with 80% acetone (4.5 mL). Samples absorbance was taken at 645, 663, and 470 nm using spectrophotometer (Shimadzu, Japan).

Proline estimation

Proline was estimated in different parts of *P. hydropiper* using procedure of Bates et al. (1973). Fresh sample (100 mg each) was properly homogenized in 2-mL microcentrifuge tubes having 3% (w/v) sulfosalicylic acid (1.5 mL).The homogenate obtained was subjected to centrifugation (13,000 rpm) for 5 min. The supernatant was added to 2 mL each of acid ninhydrin and glacial acetic acid in clean tubes. Then the resulting mixture was kept for 1h at 100 °C in water bath. Reaction tubes were quickly immersed in ice cooled water to end the reaction. Subsequently, toluene (1 mL) was added to each tube and thoroughly mixed for 30 s by vortexing. Then chromophore layer containing toluene was taken into clean tubes and heated to room temperature. Spectrophotomer (Shimadzu, Japan) was used to measure absorbance at 520 nm of each sample. Toluene was taken as control (blank). For estimation of proline in various samples, calibration curve of standard proline was used.

Phenolic and flavonoid estimation

Total phenolics and total flavonoids in different tissues of *P. hydropiper* were estimated by colorimetric methods. For extract preparation, each plant sample (300 mg) was properly dissolved in 100% methanol (1.5 mL) by two-time sonication and vortexing for 30 min. Subsequently, the mixture was subjected to centrifugation (13,000 rpm) for 5 min. The supernatants were isolated and later on used in biochemical analysis (Zahir et al. 2014). To estimate total phenolics, the procedure of Velioglu et al. (1998) was adopted using Folin-Ciocalteu (FC) reagent. Total flavonoids were estimated by colorimetric method of Chang et al. (2002) using aluminum chloride. For total phenolic and total flavonoid analysis, spectrophotometer (Shimadzu, Japan) was used to measure absorbance at 630 nm and at 450 nm respectively. Phenolic and flavonoid contents were expressed as equivalent of gallic acid and quercetin respectively.

Antioxidant activity determination

The antioxidant potential of different parts of *P. hydropiper* was assessed by the method of Ahmad et al. (2010) with a stable free radical DPPH (1,1-diphenyl-2-picrylhydrazyl). To measure absorbance at 517-nm wavelength of reaction solution of different samples, UV-visible spectroscopy (Shimadzu, Japan) was used. The antioxidant activities were assessed as percentage discoloration of DPPH solution as shown in given equation: DPPH free radical scavenging activity (%) = $[A_c - A_s/A_c] \times 100$

where A_S= absorbance of sample, A_C=absorbance of DPPH solution (Control).

Phenyl ammonia lyase activity determination

Phenyl ammonia lyase (EC 4.3.1.24) (PAL) activity was assessed using method of Khan et al. (2016). Fresh plant tissues (100 mg each) were thoroughly homogenized in ice chilled potassium borate buffer (100 mM) (pH 8.8) including mercaptoethanol (2 mM). The homogenate was centrifuged (12,000 rpm) at 4 °C for 10 min. Supernatants were collected and used in enzymatic assays. Two-milliliter reaction solution included [1 mL potassium borate buffer (100 mM) at pH 8.8, 0.5 mL phenylalanine (4 mM), and plant extract (0.5 mL)]. The absorbance was recorded at 290-nm wavelengths before and after incubation at 30 °C for 30 min by spectrophotometer (Shimadzu, Japan) and the reaction was stopped using 6M HCl (0.2 mL). Product (t-cinnamic acid) formation was monitored by increase in absorbance values of different plant samples.

Antioxidant enzyme activity determination

To monitor antioxidant enzyme activities in different samples, plant extracts were prepared according to procedure of Nayyar and Gupta (2006) with slight modifications. Fresh samples (100 mg each) of leaves, stems, and roots were thoroughly

homogenized in potassium phosphate buffer (1 mL, 50 mM) fortified with 1% PVP maintained at pH 7. The homogenate was centrifuged (14000 rpm) at 4°C for 30 min. The supernatant was isolated and later on used in enzymatic assays. Superoxide dismutase (SOD; EC 1.15.1.1) activity was determined with the established procedure of Giannopolitis and Ries (1977). Similarly, peroxidase (POD; EC 1.11.1.7) activity was assessed with the procedure of Lagrimini (Lagrimini 1991). Ascorbate peroxidase activity (APx; EC 1.11.1.11) was determined by the protocol of Miyake et al. (2006).

Lead analysis

For Pb analysis, plant samples were subjected to acid digestion according to protocol of Allen et al. (1974). Dry powder (0.25 g each) of plant tissues was added to acid solution (6.5 mL) containing sulfuric acid, perchloric acid, and nitric acid (Sigma) (1:0.5:5) in flasks (50 mL). Then plant samples were thoroughly digested on electric hot plate, when white fumes were formed inside the flasks. Following acid digestion, samples were cool down to room temperature and subsequently, filtrates were isolated in clean flasks. Filtrate volume was then made up to 50 mL using distilled water and stored for Pb estimation. Pb content in different plant tissues was estimated using inductively coupled plasma spectroscopy (Perkin Elmer, USA).

Phytoremediation efficacy of plants

Phytoremediation efficacy of plants mainly depends on metal accumulation and their subsequent translocation into aerial parts which are indicated by bioconcentration and translocation factors. Bioconcentration factor was defined by the ratio of metal content in plant tissues to that in the medium, while translocation factor was measured as the ratio of metal content in plant shoots to roots and demonstrates plant ability to translocate metal from roots toward shoots (Liang et al. 2017).

Statistical analysis

All treatments and control experiments were performed in triplicates and data was statistically analyzed through ANOVA. Mean values of treatments were compared by Tukey's multiple comparison test ($P \leq 0.05$). Results were expressed as mean±standard error of replicates. GraphPad (version 5) was used for statistical analysis and graphical presentation was made with OriginPro 8.5. Pearson's correlation (1-tailed) at $P \leq 0.05$ as significant was employed to determine correlation among the selected morphological and biochemical parameters of *P. hydropiper*.

Results and discussion

Characterization of ZnO nanoparticles

UV-visible spectroscopy

UV-vis spectroscopic techniques are commonly used to monitor synthesis and stability of nanoparticles in aqueous solutions (Anjum and Abbasi 2016). The color variations from dark green to light brown of nanoparticle suspension indicated biosynthesis of ZnO NPs (Fig. S1, Supplementary Material). The UV-visible profiles showed maximum absorption peak at 378-nm wavelength (Fig. S2 a, b, Supplementary Material). These findings match to the characteristic banding pattern of ZnO NPs (Sharmila et al. 2019). For the stability of ZnO NPs, periodical UV-visible spectroscopy was performed for 2 months. The results revealed optimum absorption spectra at the same wavelength which reflects stable nature of the synthesized ZnO NPs (Fig. S2c, Supplementary Material). Similar findings were also reported for callus mediated biosynthesis of silver nanoparticles (Anjum and Abbasi 2016).

XRD and FTIR analysis

To assess crystallite size and phase purity of biosynthesized ZnO NPs, X-ray diffraction (XRD) analysis was carried out. The spectrum showed distinct diffraction peaks of 2 theta values at 31.44°, 34.41°, 36.53°, 47.55°, 56.34°, 62.83°, and 67.62° which could be indexed to (100), (002), (101), (102), (110), (103), and (112) reflection planes respectively as depicted in the blueprint of XRD (Fig. S3a). The obtained XRD pattern matches to the hexagonal wurtzite crystal structure of zinc oxide (JCPDS card No: 36-1451) (Jabeen et al. 2017). Moreover, the crystalline nature of the samples was portrayed by the sharp and intense diffraction peaks as shown in Fig. S3a (Supplementary Material). The absence of extra diffraction peaks in addition to ZnO confirms impurities free synthesis of highly purified ZnO NPs. The average particle size of ZnO NPs was determined via Scherrer's equation and found to be 17.91 nm. These findings are comparable with previous results of Kalpana et al. (2018).

Fourier transform infrared (FTIR) spectroscopic analysis was performed to identify possible functional groups of various phytochemicals in leaf extract which may help in reduction and stabilization of ZnO NPs. FTIR profile of ZnO NPs shows absorption peaks approximately at 3308.82 cm^{-1}, 2950.12 cm^{-1}, 2853.21 cm^{-1}, 1740.93 cm^{-1}, 1582.81 cm^{-1}, 1367.31 cm^{-1}, 1025.48 cm^{-1}, and 537.09 cm^{-1} for ZnO NPs (Fig. S4, Supplementary Material). The wider band at 3308.82 cm^{-1} designates vibration stretches of O-H and N-H in phenols, flavonoids, alcohols, and protein (Adil et al. 2019; Mittal et al. 2014). Similarly, peak appeared at 2950.12 cm^{-1} shows C-H stretching in aromatic compounds (Jyoti et al. 2016).

Likewise, the peak at 2853.21 cm^{-1} matches to O-H stretch in carboxylic acids (Anjum and Abbasi 2016). The sharp peak at 1740.93 cm^{-1} stand for C=O stretching in carboxylic acids, aldehydes, and ketones (Abbasi et al. 2017). The band at 1582.81 cm^{-1} attributes to C=C stretch in aromatic compounds (Prakash and Kalyanasundharam 2015). The frequency at 1367.31 cm^{-1} could be allocated to stretching vibrations of C-N in aromatic amines (Jamdagni et al. 2018). The strong peak recorded at 1025.48 cm^{-1} is due to C-O stretch in alcohols, ethers, and carboxylic acids (Khalil et al. 2017). The characteristic absorption band of ZnO NPs was recorded at 537.09 cm^{-1} frequency (Yedurkar et al. 2016) (Fig. S4, Supplementary Material). These findings strongly advocate the involvement of various phytochemicals in leaf extract such as phenolics, flavonoids, protein, alcohols, aliphatic amines, and carboxylic acids in biosynthesis as well as stabilization of ZnO NPs (Umar et al. 2019).

SEM and EDX analysis

Shape, size, and surface morphology of leaf extract–mediated ZnO NPs were assessed by scanning electron microscopy as illustrated in Fig. S5a (Supplementary Material).The SEM micrographs clearly depicted the existence of both well-scattered individual ZnO NPs and numerous agglomerated particles. The synthesized ZnO NPs appear almost spherical-shaped beads like structures with mean diameter of 17.83 nm. Similar round-shaped aggregates for ZnO NPs were previously reported by many researchers (Pal et al. 2018; Emad et al. 2017). The elemental profile and chemical purity of ZnO NPs were analyzed by energy dispersive X-ray spectroscopy (EDX) as depicted in Fig. S5b (Supplementary Material). The sharp peaks in the region (0.0–2.0 keV) corresponding each to zinc and oxygen, while the two relatively shorter peaks in range (8.0–10.0 keV) represents metallic zinc in the samples (Fig. S5b, Supplementary Material). The EDX results further validated synthesis of ZnO NPs in its pure form.

DLS analysis

Size and surface charge distribution play a pivotal role in stability and biological activities of nanoparticles. To determine particle size of colloidal solutions, DLS technique is widely employed to assess time-dependent fluctuations in scattered light of nanoparticle suspensions because of their Brownian motion, which mainly rely on particle hydrodynamic size (Bhattacharjee 2016). In this study, hydrodynamic sizes of ZnO NPs in liquid growth medium were found 41.2 nm as indicated in Fig. S6a (Supplementary Material). The bigger sizes of ZnO NPs in liquid medium in comparison to both XRD and SEM sizes might be attributable to the presence of ions or phyto chemicals such as capping and stabilizing agents adhered to surfaces of ZnO NPs in liquid medium. These findings endorsed previous investigations (Ahamed et al. 2011).

Zeta potential (ζ) is considered a typical measure to express surface charge and stability of particles in colloidal solutions. Suspensions which exhibit $|\zeta| \geq 15$ mV are usually classified as stable colloids (Modena et al. 2019).

Currently, ZnO NPs dispersed in liquid growth medium showed −28.4 mV zeta potential which indicate a stable nanoparticle suspension as portrayed in Fig. S6b (Supplementary Material). The negative charge on particle surface is due to the adsorption of negatively charged poly phenols on metal ions found in leaf extract which help in particle dispersion and thus hinder them from agglomeration (Vimala et al. 2014).

Plant growth and biomass accumulation

The current study was undertaken to overcome phytotoxicity of (Pb) in seedlings of *P. hydropiper* under hydroponic culture by applying ZnO NPs. Previously, numerous higher plants have been screened for tolerance and hyper accumulation of Pb in order to find out candidate plants for the restoration of lead-polluted regions (Andra et al. 2009). ZnO NP effect on different morphological attributes in *P. hydropiper* under Pb stress is shown in Table 1. Pb stress significantly halted plant growth (stem and root length), biomass (fresh and dry), and total water content in plant parts and entire plant when Pb-treated plants (C1) were compared to plants grown in Pb-free medium (C) (Table 1). To assess plant growth under metals stresses, visual observation of plant height and biomass accumulation are considered as the most prominent indicators (Rizwan et al. 2017). Heavy metal stress is often associated with plant growth inhibition in a wide range of plant species grown in polluted soil and water (Gong et al. 2019; Ullah et al. 2018). Plant growth retardation by metal stress is due to water deficit resulting from disturbance of water balance (Ekmekçi et al. 2009). The Pb is among the most abundant and highly phytotoxic heavy metals across the globe, and its pollution causes significant and irreversible loss to plant growth and productivity (Qin et al. 2018). For efficient phytoremediation of metal-polluted soils, it is imperative to identify native metal hyper accumulator plants producing high biomass and possessing high metal tolerance potentials (Lajayer et al. 2017). All tested concentrations of ZnO NPs improved plant growth and biomass accumulation. However, maximum plant height (18.23±0.46 cm), root length (8.33±0.20 cm), fresh biomass (3.69±0.12, 5.13±0.10, 3.45±0.11, and 12.27±0.32 g), and dry biomass (1.62±0.07, 2.22±0.09, 1.27±0.07, and 5.11±0.21 g) of leaves, stems, root, and entire plant respectively were recorded under T3 (15 mg L^{-1} ZnO NPs) (Table 1). Moreover, growth of *P. hydropiper* was suppressed at elevated level (20 mg L^{-1}) of ZnO NPs (Table 1). Earlier studies of Faizan et al. (2018) and Pullagurala et al. (2018) reported positive effects of ZnO NPs on growth of different

Table 1 Effects of ZnO nanoparticles on growth and biomass of *P. hydropiper* plantlets grown under lead stress in hydroponic culture

Treatments	Length (cm)±SE		Fresh biomass (g) ±SE				Dry biomass (g) ±SE				Total water content (g) ±SE			
	Stem	Root	Leaves	Stem	Roots	Entire plant	Leaves	Stems	Roots	Entire plant	Leaves	Stems	Roots	Entire plant
C	16.52±0.46^{b}	7.35± 0.29^{b}	2.87± 0.10^{b}	4.57±0.18^{b}	2.69±0.14^{b}	10.13±0.42^{b}	1.32± 0.12^{b}	2.13±0.09^{a}	1.16±0.05^{a}	4.60±0.25^{b}	1.55± 0.04^{b}	2.45±0.09^{b}	1.54±0.09^{b}	5.53± 0.17^{b}
C1	10.66±0.34^{f}	5.40± 0.14^{c}	1.58± 0.11^{e}	2.66±0.09^{e}	1.31±0.08^{d}	5.55± 0.10^{d}	0.84± 0.09^{d}	0.92±0.08^{c}	0.66±0.04^{e}	2.41±0.19^{d}	0.74± 0.01^{c}	1.74±0.01^{c}	0.65±0.12^{d}	3.14± 0.10^{d}
T1	13.20±0.18^{e}	5.96± 0.19^{c}	2.54± 0.09^{d}	3.65±0.11^{d}	1.84 ±0.11^{cd}	8.04± 0.19^{c}	0.96± 0.08^{c}	1.45±0.06^{b}	0.71±0.04^{e}	3.12±0.11^{c}	1.58± 0.04^{b}	2.20±0.14^{b}	1.13±0.09^{c}	4.92± 0.24^{c}
T2	15.16±0.23^{c}	6.82± 0.28^{bc}	2.78± 0.11^{c}	3.72±0.13^{d}	2.03±0.13^{c}	8.53± 0.13^{c}	1.29± 0.15^{b}	1.60±0.08^{b}	0.86±0.06^{c}	3.76±0.20^{c}	1.49± 0.05^{b}	2.12±0.05^{b}	1.16±0.07^{c}	4.77± 0.07^{c}
T3	18.23±0.46^{a}	8.33± 0.20^{a}	3.69± 0.12^{a}	5.13±0.10^{a}	3.45±0.11^{a}	12.27±0.32^{a}	1.62± 0.07^{a}	2.22±0.09^{a}	1.27±0.07^{a}	5.11±0.21^{a}	2.07± 0.07^{a}	2.91±0.01^{a}	2.18±0.04^{a}	7.16± 0.12^{a}
T4	14.22±0.45^{d}	6.36± 0.23^{bc}	2.77± 0.05^{c}	3.89±0.08^{c}	2.35±0.06^{b}	9.01± 0.18^{bc}	1.07± 0.08^{c}	1.71±0.08^{ab}	0.94±0.06^{b}	3.71±0.23^{c}	1.70± 0.03^{b}	2.18±0.01^{b}	1.41±0.01^{b}	5.29± 0.04^{b}

Pb lead, *SE* standard error, *cm* centimeter, *g* gram, *ppm* part per million, *ZnO* zinc oxide, *NPS* nanoparticles, *T* treatment. Values are expressed as means ± standard error of the triplicates (n=3). Different alphabets in superscript denote significant difference among treatments at $P \leq 0.05$ using Tukey's multiple comparison test. C (Control without Pb), C1 (Control with Pb: 50 mg L^{-1}), T1 (50 mg L^{-1} Pb+ 5 mg L^{-1} ZnO NPS), T2 (50 mg L^{-1} Pb+10 mg L^{-1} ZnO NPS), T3 (50 mg L^{-1} Pb+15 mg L^{-1} ZnO NPS), and T4 (50 mg L^{-1} Pb+20 mg L^{-1} ZnO NPS)

plant species up to certain optimum concentration. The ZnO NPs furnish Zn^{2+}, which is an essential micronutrient to sustain plant growth and metabolic activities (Liu et al. 2015).

These results indicated that ZnO NPs alleviated Pb stress by stimulating plant growth and biomass production and thus induced metal stress resistance in plants (Venkatachalam et al. 2017a). Previously, Jabeen et al. (2017) reported boosted growth of *Lycopersicon esculentum* L. seedlings at lower dose of ZnO NPs while higher concentrations hindered growth of plantlets. Likewise, in another study, *Gossypium arboreum* L. growth was improved in dose-dependent pattern with ZnO NPs (Priyanka and Venkatachalam 2016). The promotion in growth of *P. hydropiper* plantlets treated with ZnO NPs might be due to better bioavailability of water and essential nutrients for enhanced plant uptake (Jabeen et al. 2017). The inhibition of plant growth at higher concentrations of nanoparticles could be ascribed to nanoparticle aggregation on root surface to interrupt root respiration and nutrient uptake (Gong et al. 2019). Under in vitro conditions, growth of *Cicer arietinum* L. and *Vigna radiata* L. was considerably enhanced with lower concentration of ZnO NPs while higher concentration decreased seedling growth (Mahajan et al. 2011). Previously, ZnO NPs applied to soil (0, 25, 50, 75, and 100 mg kg^{-1}) and as foliar spray (0, 25, 50, 75, 100 mg L^{-1}) significantly increased plant growth and activities of antioxidant enzymes while decreased Cd accumulation in a dose-dependent pattern for *Triticum aestivum* L. (Hussein and Abou-Baker 2018).

Photosynthetic pigments

The response of chlorophyll a, b and carotenoids in leaves under ZnO NPs is given in Fig. 2a. Photosynthetic pigments were adversely affected in Pb-treated plants (C1) in reference to control plants without Pb exposure (C) (Fig.2a). Plant exposure to toxic heavy metals results in oxidative stress due to increased production of ROS, which damages several vital biomolecules including nucleic acids, proteins, and lipids inside the cells (Singh et al. 2013). The content of photosynthetic pigments could serve as an important bio indicator of heavy metal-induced toxicity in plants. The reduction in chlorophyll contents in leaves of metal-treated plants might be due to oxidation of photosynthetic pigments (Ma et al. 2015). Application of ZnO NPs enhanced chlorophyll and carotenoid content, but highly significant increase in chlorophyll a (37.78±1.05 μg/g) was found at T3 (15 mg L^{-1}), chlorophyll b (18.48±1.44μg/g) at T2 (10 mg L^{-1}), and carotenoid content (14.94±1.04 μg/g) under T1 (5 mg L^{-1}) (Fig. 2a).

Variations in total chlorophyll, Chl a & b ratio under ZnO NP treatments, are shown in Fig. 2b.Total chlorophyll synthesis was severely inhibited in plants treated with Pb (C1) relative to control plants (C) (Fig. 2b). Furthermore, total chlorophyll exhibited linear increase with increasing concen-

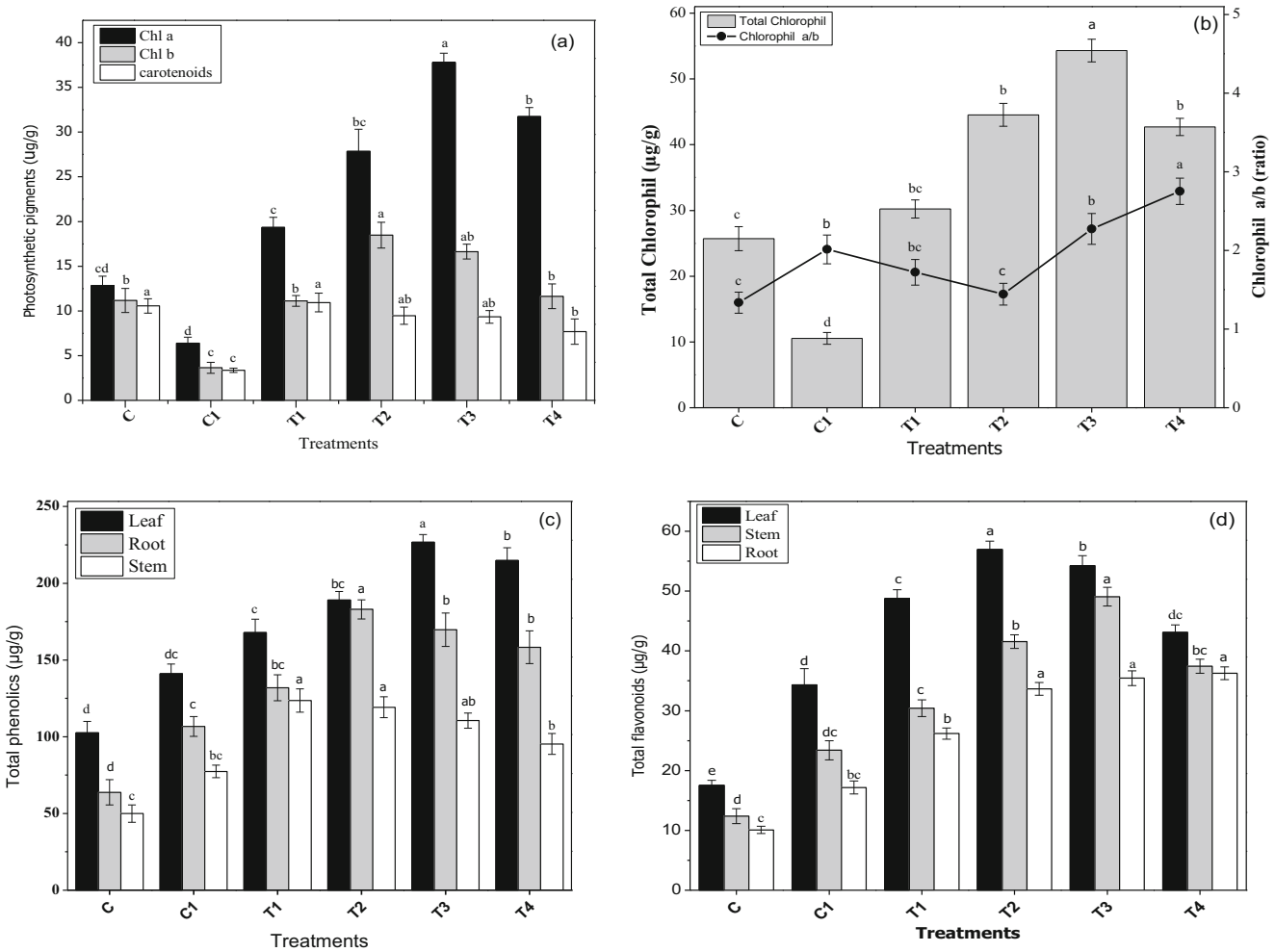

Fig. 2 Photosynthetic pigments (a), total chlorophyll content and chlorophyll a and b ratio (b), total phenolic content (c), and total flavonoid content (d) in response to ZnO nanoparticle treatments. Values are expressed as means ± standard error of the triplicates (n=3). Bars with different alphabets denote significant difference among treatments at $P \leq 0.05$ using Tukey's multiple comparison test. C (Control without Pb), C1 (Control with Pb: 50 mg L^{-1}), T1 (50 mg L^{-1} Pb+ 5 mg L^{-1} ZnO NPS), T2 (50 mg L^{-1} Pb+10 mg L^{-1} ZnO NPS), T3 (50 mg L^{-1} Pb+15 mg L^{-1} ZnO NPS), and T4 (50 mg L^{-1} Pb+20 mg L^{-1} ZnO NPS)

tration of ZnO NPs, but the highest increase (54.32±1.72µg/g) was reported at T3 (15 mg L^{-1}) under Pb stress (Fig. 2b). In current study, ZnO NPs at higher concentration T4 (20 mg L^{-1}) inhibited total chlorophyll content in leaves of *P. hydropiper* (Fig. 2b). Earlier studies reported that ZnO NPs at lower dose significantly augmented chlorophyll and carotenoids in *T. aestivum* (Solanki 2018), *Cenchrus americanus* L. (Tarafdar et al. 2014), *C. arietinum* (Hajra and Mondal 2017), and *Cyamopsis tetragonoloba* L. (Raliya and Tarafdar 2013).

Phenolic and flavonoid contents

Phenolic and flavonoid profile in response to ZnO NPs treatments is shown in Fig. 2c and d respectively. Phenolic contents in various plant parts were enhanced upon exposure to Pb treatment (C1) (Fig. 2c). Similarly, increased phenolic content was found in *Parthenium hysterophorus* L. and *Euphorbia helioscopia* L. grown on Pb-contaminated soils (Ullah et al. 2019). ZnO NPs further improved total phenolics at all tested concentrations. However, maximum TPC were recorded for leaf (226.70±5.05µg/g) in T3 (15 mg L^{-1}), for root (183.00±6.21 µg/g) in T2 (10 mg L^{-1}), and for stem (123.60±7.54 µg/g) under T1 (5 mg L^{-1}) in comparison to control with Pb only (C1). Garcia-Lopez et al. (2018) reported that ZnO NPs boosted phenolic content during germination of *Capsicum annuum* L. Contrarily, the highest dose of ZnO NPs T4 (20 mg L^{-1}) showed inhibitory effect on phenolics in various plant tissues (Fig. 2c). Earlier reports indicated that elevated levels of ZnO NPs suppressed polyphenol content in roots of *Brassica nigra* L. plantlets (Zafar et al. 2016).

The present study indicated that Pb stress (C1) highly induced total flavonoid synthesis in leaves, stems, and roots of the plants (Fig. 2d). To alleviate heavy metal stress, plants trigger their antioxidative defense system including phenolics and flavonoids which function as metal chelators and natural

scavengers of ROS which protect plants against oxidative stress (Ilboudo et al. 2012; Michalak 2006). In current study, optimum contents of flavonoids in leaves (56.97±1.37 μg/g) were reported at T2 (10 mg L^{-1} ZnO NPs), in stems (49.07±1.55 μg/g) at T3 (15 mg L^{-1} ZnO NPs), and in roots (36.26±1.06 μg/g) at T4 (20 mg L^{-1} ZnO NPs) as shown in Fig. 2d. These results correlate with findings of Zafar et al. (2016) who conveyed a dose-dependent increase in flavonoids with ZnO NPs in seedlings of *B. nigra*. Flavonoid content was comparatively higher in leaves, moderate in stems, and minimum in roots (leaves > stems > roots) of *P. hydropiper* plantlets (Fig. 2d).

Antioxidant activity and proline content

Antioxidant potential using DPPH free radical scavenging assay in different plant tissues under ZnO NP treatments is presented in Fig. 3a. Current results revealed that antioxidant activity in plant tissues was boosted in Pb-exposed plants (C1) relative to control (C) (Fig. 3a). Plants develop resistance to metal stress by inducing secondary metabolite accumulation and certain antioxidant enzymes to counteract oxidative damages of cellular components and biomolecules caused by highly reactive free radicals (Na and Salt 2011). Similarly, DPPH antioxidant capacity of *Gynura procumbens* (Lour.) Merr. was significantly increased in plants treated with copper and cadmium (Ibrahim et al. 2017). In present study, ZnO NPs displayed a dose-dependent response of antioxidant activity up to some extent in various plant tissues. Leaves and roots exhibited maximum (84.48±3.06 and 51.19±1.29%) antioxidant activity in T3 (15 mg L^{-1} ZnO NPs), while stems showed best antioxidant response (67.88±2.23%) at T2 (10 mg L^{-1} ZnO NPs) under hydroponic culture (Fig. 3a). These results endorsed previous findings of Singh et al. (2018); they found a positive impact of ZnO NPs on antioxidant activity in *B. nigra*. Likewise, proline content was also enhanced in leaves, stems, and roots when plants were exposed to Pb stress (Fig. 3b).

Plants being sessile organisms are constantly facing an array of environmental stresses including toxic heavy metals. To withstand metal stress, plants accumulate a variety of metabolic products mainly proline to nullify toxic effects of heavy metals (Hayat et al. 2012). Amino acid proline plays an essential role

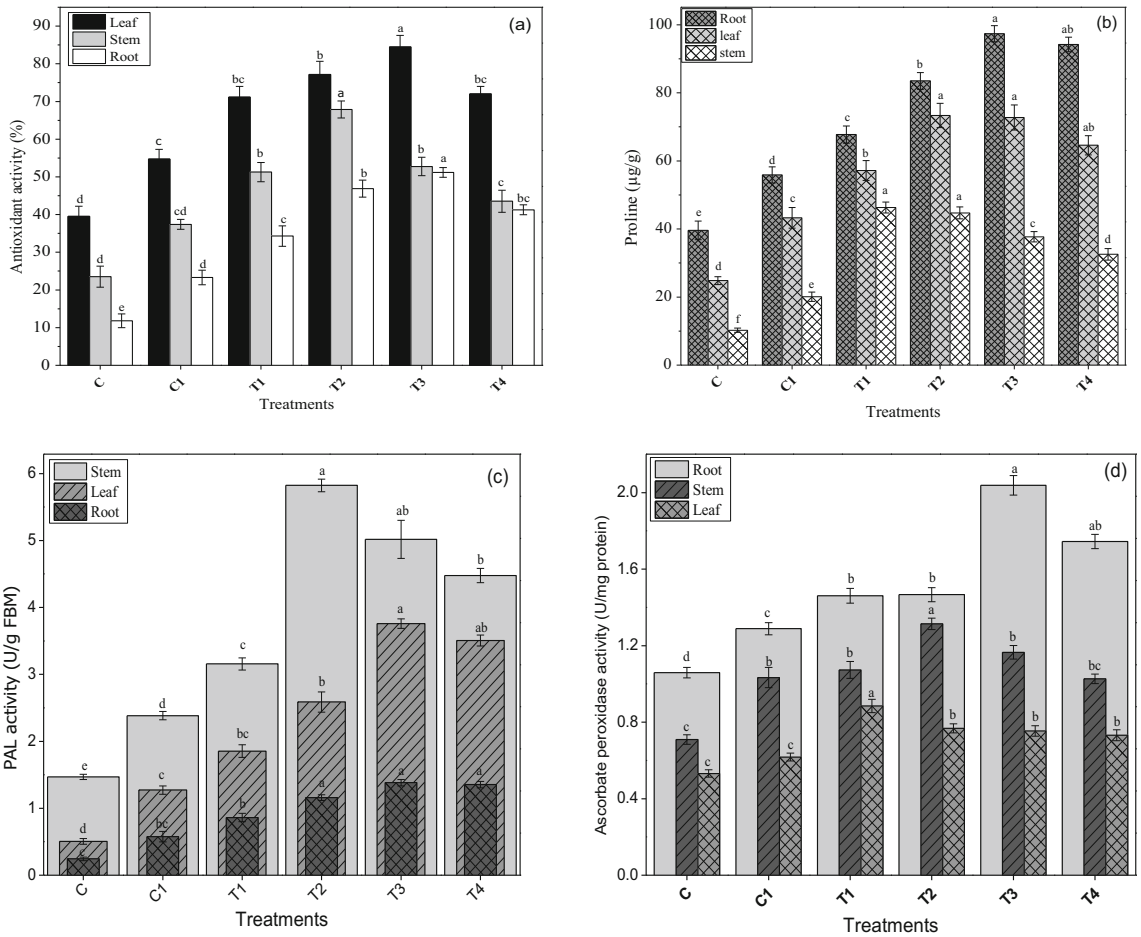

Fig. 3 Free radical scavenging activity (a), proline content (b), phenyl ammonia lyase (PAL) activity (c), and ascorbate peroxidase (APx) activity (d) in response to ZnO nanoparticle treatments. Values are expressed as means ± standard error of the triplicates (n=3). Bars with different alphabets denote significant difference among treatments at $P \leq 0.05$ using Tukey's multiple comparison test

in plant tolerance against stressful conditions and may act as osmoregulator, metal chelator, quencher of ROS; stabilizes; and protects enzymes (Choudhary et al. 2007). Proline content was significantly improved in various parts of *P. hydropiper* in response to all tested doses of ZnO nanoparticles. But the highest proline content was observed in roots (97.37±2.38 μg/g) at T3 (15 mg L^{-1} ZnO NPs), in leaves (73.33±3.56 μg/g) at T2 (10 mg L^{-1} ZnO NPs), and in stem (46.29±1.61 μg/g) at T1 (5 mg L^{-1} ZnO NPs) (Fig. 3b). Proline content was comparatively more in roots, intermediate in leaves, and minimum in stems of plants (roots>leaves>stems) (Fig. 3b), whereas ZnO NPs at maximum dose (20 mg L^{-1}) significantly reduced proline contents in various plant parts. These findings are consistent with the work of Dogaroglu and Koleli (2017); they found that proline content was enhanced with increasing concentration of ZnO NPs in *T. aestivum*.

Phenyl ammonia lyase and ascorbate peroxidase activity

The differential effect of ZnO NPs on phenyl ammonia lyase (PAL) activity in various plant parts is shown in Fig. 3c. Relatively higher PAL activity was observed in stem, intermediate for leaves, and lowest in roots of ZnO NPs treated and control plants of *P. hydropiper* (Fig. 3c). Phenyl ammonia lyase is one of the crucial strategic enzymes engaged in plant defense against biotic and abiotic stresses (Astaneh et al. 2018). It is the first regulatory enzyme required in synthesis of secondary metabolites particularly phenolics and flavonoids during phenylpropanoid pathway. This enzyme is responsible for reversible deamination of L-Phenylalanine into trans-cinnamic acid that acts as precursor for biosynthesis of phenolic and flavonoid compounds which scavenge ROS produced in plants during stresses (Smirnov et al. 2012). Therefore, PAL plays a fundamental role in plant combat against heavy metal stresses including Pb (Pawlak-Sprada et al. 2011). The Pb treatment (C1) positively affected PAL activity in different parts of plants in comparison to control without Pb (C). Similar pattern of PAL activities were also reported in *Lactuca sativa* L. under cadmium exposure (Kosyk et al. 2017). Likewise, varying concentrations of ZnO NPs enhanced PAL activity under Pb stress in reference to control (C1). Current study indicated that the highest PAL activity was found in stems (5.82±0.09 U/g FBM) at T2 (10 mg L^{-1} ZnO NPs), for leaves (3.76±0.07 U/g FBM), and roots (1.38±0.05 U/g FBM) in T3 (15 mg L^{-1} ZnO NPs) in seedlings of *P. hydropiper* (Fig. 3c). Iranbakhsh et al. (2018) observed improved PAL activity in roots and leaves of ZnO NP-treated plantlets of *C. annuum* under in vitro conditions.

The Pb stress (C1) augmented ascorbate peroxidase (APx) activity in roots and stems, while in leaves, comparable APx activity was reported relative to control (C) (Fig. 3d). Heavy metal toxicity in plants induces excessive accumulation of ROS which trigger antioxidative enzymes to eliminate these ROS and thus protect plants against oxidative damage (Smirnov et al. 2012). Different treatments of ZnO NPs improved APx activity in plant tissues under hydroponic culture. However, highly significant increase was perceived for roots (2.04±0.05 U/mg protein) in T3 (15 mg L^{-1} ZnO NPs), for stem (1.31±0.03 U/mg protein) in T2 (10 mg L^{-1} ZnO NPs), and for leaves (0.88±0.03 U/mg protein) in T1 (5 mg L^{-1} ZnO NPs) (Fig. 3d). Similar increase in ascorbate peroxidase activity was reported in *L. esculentum* seedlings in response to ZnO nanoparticles alone or when fortified with 24-epibrassinolide (Li et al. 2016).

Superoxide dismutase and peroxidase activity

Plants under heavy metal stress produce elevated levels of highly reactive oxygen species which negatively affect plant cellular metabolisms through oxidative stress and cell damages (Choudhury et al. 2013). To combat stresses, plants are equipped with well-organized defense mechanism consisted of antioxidative enzymes like superoxide dismutase, peroxidase, and ascorbate peroxidase, which eradicate ROS and thus circumvent oxidative damage (Gong et al. 2017). Superoxide dismutase is the first antioxidant enzyme, which predominantly transforms highly reactive superoxide anion ($O_2^{\cdot-}$) into relatively less reactive hydrogen peroxide (H_2O_2). Similarly, peroxidase is also involved in conversion of toxic hydrogen peroxide (H_2O_2) into water molecules (Ma et al. 2015). Superoxide dismutase (SOD) activity in different parts of *P. hydropiper* under ZnO NP treatments is given in Fig. 4a. In plant tissues (leaves, stems, and roots), SOD activity was increased with Pb exposure (C1) relative to plants without Pb stress (C). Similarly, SOD activity was also greatly enhanced in Pb-treated *Vallisneria natans* L. seedlings (Wang et al. 2012). In stems and roots, the highest SOD activity (1.67 ±0.06 and 0.48±0.02 U/mg protein) respectively was found in T2 (10 mg L^{-1} ZnO NPs). Likewise, ZnO NPs in leaves also increased enzymatic activities in a dose-dependent manner and maximum values (1.15±0.09 U/mg protein) were recorded in T3 (15 mg L^{-1} ZnO NPs). Moreover, ZnO NPs at 20 mg L^{-1} dose (T4) inhibited SOD activity in various tissues of *P. hydropiper* (Fig. 4a). Previously, comparable trend in SOD activity was observed in *Gossypium hirsutum* L. leaves treated with ZnO NPs (Venkatachalam et al. 2017b). Effects of ZnO NP treatments on peroxidase (POD) activity in leaves, stems, and roots of *P. hydropiper* are shown in Fig. 4b. In present study, Pb stress (C1) significantly enhanced peroxidase activity in different parts of *P. hydropiper* relative to control (C). Lou et al. (2017) reported that POD activity was highly increased in *Festuca arundinacea* (Schreb.) plants grown in Pb and cadmium-polluted media. Various treatments of ZnO NPs stimulated peroxidase activity in plant parts when

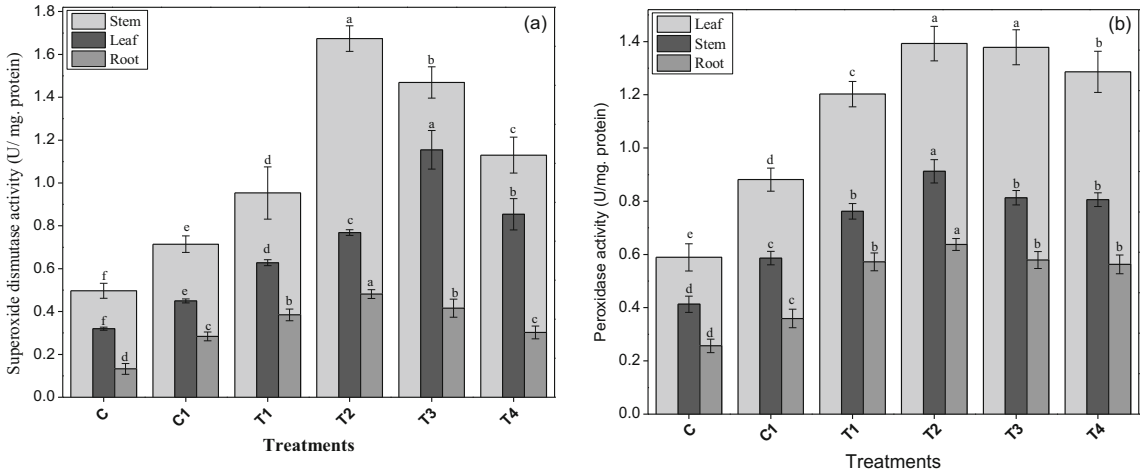

Fig. 4 Superoxide dismutase's activity (a) and peroxidase activity (b) in response to ZnO nanoparticle treatments. Values are expressed as means ± standard error of the triplicates. Bars with different alphabets denote significant difference among treatments at $P \leq 0.05$ using Tukey's multiple comparison test

compared to control (C1). These findings indicated that ZnO NPs at moderate concentration T2 (10 mg L^{-1}) resulted in optimum activity of peroxidase in leaves (1.39±0.06 U/mg protein), stem (0.91±0.04 U/mg protein), and roots (0.64 ±0.02 U/mg protein) (Fig. 4b). However, highest tested concentration (20 mg L^{-1}) of ZnO NPs (T4) caused a decline in POD activity of *P. hydropiper* plant parts (Fig. 4b). These results conform to previous work of Venkatachalam et al. (2017b) who detected higher POD activity in *G. hirsutum* treated with ZnO NPs under lead stress. The decreasing trend in antioxidant enzyme activities at the highest ZnO NP concentration (20 mg L^{-1}) could be attributed to enzyme inhibition due to increased accumulation of free radicals in stressed plant tissues (Malar et al. 2016).

Lead accumulation and translocation

The Pb concentration, accumulation, and translocation in different parts and in entire plant of *P. hydropiper* under ZnO NP treatments are depicted in Table 2 and Fig. 5a, b respectively. The Pb concentration in different plant parts and in entire plant was significantly increased with ZnO NP application as compare to control with Pb only (C1) (Table 2 and Fig. 5a). Maximum Pb content in leaves and roots (92.00±3.22 and 255.60±4.80 mg kg^{-1}) and entire plant (471.67±7.8 mg kg^{-1}) respectively was found in T3 (15 mg L^{-1} ZnO NPs), and for stem (132.87±2.74 mg kg^{-1}) in T2 (10 mg L^{-1} ZnO NPs) treatment. Moreover, the highest level of ZnO NPs (20 mg L^{-1}) decreased Pb concentration in different tissues and entire experimental plant (Table 2 and Fig. 5a). In this study, Pb accumulation in various plant tissues and entire plant was highly improved with ZnO NP treatments relative to control (C1). The accumulation of Pb in *P. hydropiper* tissues and entire plant was enhanced with increasing concentrations of ZnO NPs. However, the highest Pb accumulation was observed at 15 mg L^{-1} ZnO NP treatment (T3) both in plant parts and entire plants of *P. hydropiper* (Table 2 and Fig. 5b). ZnO NPs at 20 mg L^{-1} (T4) significantly declined Pb accumulation both in plant tissues and entire plants (Table 2 and Fig. 5b). The decreasing trend of Pb accumulation might be due to toxicity of ZnO NPs in plants at elevated concentrations, which suppressed plant growth, and ultimately impeded Pb uptake efficiency (Gong et al. 2017). Similarly, Venkatachalam et al. (2017b) reported enhanced uptake of cadmium in seedlings of *Leucaena leucocephala* (Lam.) de Wit. treated with ZnO NPs. Huang et al. (2018) found that zero-valent iron at nanoscale range significantly increased Pb phytoaccumulation at relatively lower dose in *Lolium perenne* L. cultivated in river sediment. Gul et al. (2018) described that TiO_2 NPs supported Cd phytoextraction in *Pelargonium hortorum* L. grown under soil conditions.

Highly variable response was observed for percentage Pb distribution in different plant tissues under ZnO NP treatments; however, reasonably higher Pb accumulation (%) was recorded in stems except T3 (15 mg L^{-1} ZnO NPs). Relatively higher Pb translocation from roots to stems rather than leaves was recorded in response to different doses of ZnO NPs. Furthermore, ZnO NPs at 5 mg L^{-1} and 10 mg L^{-1} concentrations (T1 and T2) enhanced Pb translocation from root to stem in the experimental plant. All tested doses of ZnO NPs exhibited stimulatory effect on Pb bioconcentration in different tissues as well as entire plants of *P. hydropiper* (Table 2). Heavy metal translocation from plant roots to aerial parts demonstrates metal uptake capacity in various plants species. To enhance metal accumulation and its subsequent translocation into plants, aerial parts are a major challenge for plant application to effectively restore metal-polluted environment (Gong et al. 2019). The increased translocation and uptake of Pb in different parts of *P. hydropiper* when treated with ZnO NPs are a significant novel achievement of this study for

Table 2. Effects of ZnO nanoparticles on lead concentration, accumulation, distribution and translocation in different parts of *P. hydropiper* plantlets grown under lead stress in hydroponic culture.

Treatments	Pb concentration (mg/kg) ± SE			Pb accumulation (mg/ total DBM) ±SE			Pb accumulation (%) ±SE			Pb translocation ±SE		Pb bio concentration ±SE			
	Leaves	Stem	Root	Leaves	Stem	Root	Leaves	Stem	Root	R-S	R-L	Leaves	Stem	Root	Entire plant
C1	59.40±2.11^{c}	84.67±2.44^{c}	132.47±2.65^{c}	0.050±0.006^{c}	0.078±0.008^{d}	0.087±0.006^{e}	23.16±1.97^{a}	36.14±0.97^{c}	40.70±1.86^{b}	0.64±0.03^{b}	0.45±0.02^{a}	0.012±0.009^{d}	0.017±0.003^{d}	0.026±0.006^{d}	0.055±0.008^{d}
T1	72.73±2.79^{b}	106.40±2.91^{b}	165.13±2.71^{b}	0.070±0.008^{b}	0.154±0.005^{c}	0.117±0.005^{d}	20.36±1.50^{b}	45.34±1.58^{a}	34.30±0.40^{d}	0.65±0.02^{b}	0.44±0.03^{a}	0.015±0.005^{b}	0.021±0.004^{c}	0.033±0.005^{c}	0.069±0.007^{c}
T2	75.27±2.85^{b}	132.87±2.74^{a}	172.73±3.76^{b}	0.098±0.014^{ab}	0.212±0.009^{b}	0.149±0.013^{c}	21.23±2.48^{b}	46.14±1.28^{a}	32.63±3.52^{c}	0.77±0.02^{a}	0.43±0.02^{a}	0.015±0.006^{b}	0.027±0.008^{a}	0.035±0.008^{c}	0.076±0.009^{b}
T3	92.00±3.22^{a}	124.07±2.84^{ab}	255.60±4.80^{a}	0.149±0.009^{a}	0.275±0.007^{a}	0.326±0.022^{a}	19.83±0.46^{b}	36.81±0.99^{c}	43.37±0.75^{a}	0.49±0.01^{c}	0.36±0.01^{b}	0.018±0.007^{a}	0.025±0.007^{a}	0.051±0.009^{a}	0.094±0.016^{a}
T4	80.07±2.57^{b}	117.47±2.95^{b}	190.67±4.85^{ab}	0.086±0.007^{ab}	0.201±0.015^{b}	0.179±0.015^{b}	18.35±0.77^{c}	43.27±0.57^{b}	38.37±0.36^{c}	0.62±0.01^{b}	0.42±0.01^{a}	0.016±0.008^{c}	0.023±0.005^{b}	0.038±0.004^{b}	0.078±0.006^{b}

Pb lead, SE standard error, mg milligram, ppm part per million, % percentage, ZnO zinc oxide, NPS nanoparticles, T treatment, C1 control with lead only, DBM dry biomass, R-S root to stem, R-L root to leaves. Values are expressed as means ± standard error of the triplicates (n=3). Different alphabets in superscript denote significant difference among treatments at $P \leq 0.05$ using Tukey's multiple comparison test.

effective phytoremediation of metal-polluted water and soil. The results obtained demonstrated that *P. hydropiper* could be employed as a potential candidate plant to efficiently accumulate Pb and subsequently translocate it into its aerial parts from polluted environment.

Correlation analysis

Correlation among various morphological, biochemical, and physiological attributes of leaves, stem, and roots of *P. hydropiper* is described in Table S1 (a), (b), and(c) (Supplementary Material). The Pb accumulation is positively correlated with proline (r^2=0.931), phenolics (r^2=0.938), and flavonoids (r^2=0.892) in leaves (Table S1a, Supplementary Material). Similarly, in case of stem, Pb accumulation showed significant correlation with proline (r^2=0.805), phenolic content (r^2=0.823), and flavonoid content (r^2=0.995) (Table S1b, Supplementary Material). While in roots, Pb accumulation displayed strong positive relation with free proline (r^2=0.902), phenolic content (r^2=0.799), and flavonoid content (r^2=0.837) in the experimental plant (Table S1c, Supplementary Material). Similar correlation of Cd accumulation with proline and phenolics was reported in *Cannabis sativa* L. plants grown on cadmium-polluted soil (Ali et al. 2019). Ahmad et al. (2016) found enhanced proline and phenolic content in different tissues of hydroponically raised *Epilobium laxum* L. under cadmium stress. Free proline helps to scavenge ROS produced in metal-exposed plants and thus maintain normal cell functioning to minimize metal toxicity on plant growth (Sheetal et al. 2016). Elevated levels of proline and phenolics in more than 40 plants species have been reported under heavy metal stresses (Ali and Hadi 2015). Proline avoids metal stress by shielding and protecting vital enzymes from toxic metals while phenolic compounds function as natural antioxidants and prevent free radical accumulation in various stresses including heavy metals (Michalak 2006).

Conclusions

This study revealed that 15 mg L^{-1} ZnO NPs highly improved Pb concentration and accumulation in *P. hydropiper* seedlings and relieved Pb-induced stress by increasing total chlorophyll, phenolic contents, and stimulating activities of antioxidant enzymes which ultimately favored plant growth. In contrast, inhibition of plant growth, reduction in Pb accumulation, and antioxidant potentials was witnessed in *P. hydropiper* plantlets exposed to 20 mg L^{-1} ZnO NPs. Further strong positive correlation was found in Pb accumulation with proline and plant secondary metabolites in different parts of *P. hydropiper*. These findings indicated that ZnO NPs at proper concentration could significantly enhance the phytoaccumulation potential of toxic heavy metals from metal-contaminated water resources.

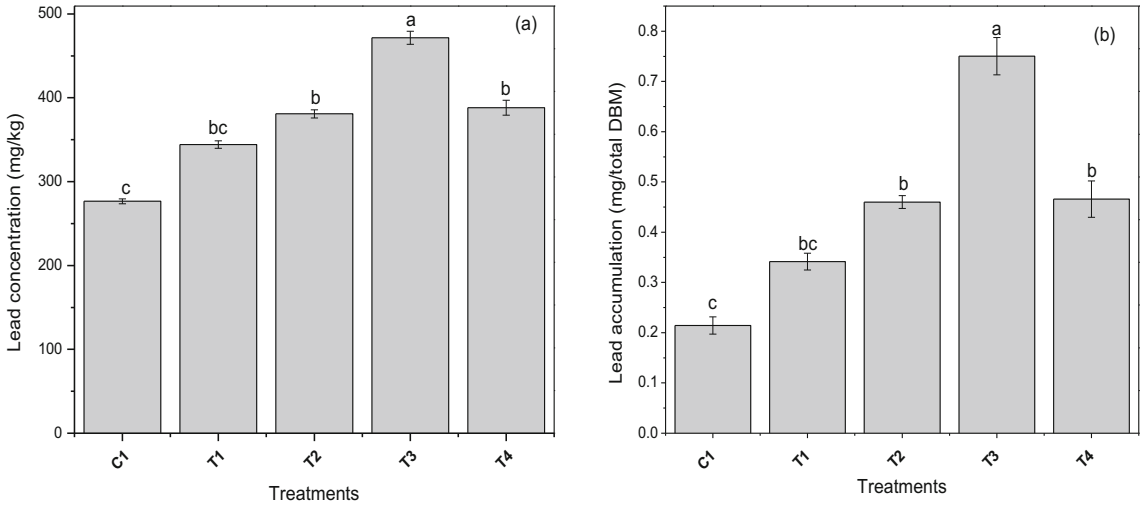

Fig. 5 Lead concentration (a) and accumulation (b) in entire plant in response to ZnO nanoparticle treatments. Values are expressed as means ± standard error of the triplicates. Bars with different alphabets denote significant difference among treatments at $P \leq 0.05$ using Tukey's multiple comparison test

Current study suggested that ZnO NPs could be employed as potential novel amendments for effective phytoremediation of Pb-polluted environment.

Supplementary Information The online version contains supplementary material available at https://doi.org/10.1007/s11356-021-13132-0.

Acknowledgements The Authors are grateful to the editor and reviewers for their valuable comments for improving this manuscript.

Author contribution FHussain contributed to experimental work and first draft write up, FHadi contributed to experimental design and edited manuscript, and QR contributed to technical aspect and provided support in characterization. Authors approved the manuscript to be published.

Funding This project was funded by the Higher Education Commission of Pakistan under indigenous PhD fellowship program via Grant No. 315-9882-2BS3-117

Data availability All data generated or analyzed during this study are included in this published article and its supplementary information files.

Declarations

Ethical approval Not applicable

Consent to participate Not applicable

Consent to publish Not applicable

Conflict of interest The authors declare no competing interests.

References

Abbasi BH, Zaka M, Hashmi SS, Khan Z (2017) Biogenic synthesis of Au, Ag and Au–Ag alloy nanoparticles using *Cannabis sativa* leaf extract. IET Nanobiotechnol 12:277–284

Adil M, Khan T, Aasim M, Khan AA, Ashraf M (2019) Evaluation of the antibacterial potential of silver nanoparticles synthesized through the interaction of antibiotic and aqueous callus extract of *Fagonia indica*. ABM Express 9:75

Ahamed M, Khan MM, Siddiqui MKJ, AlSalhi MS, Alrokayan SA (2011) Green synthesis, characterization and evaluation of biocompatibility of silver nanoparticles. Physica E Low Dimens Syst Nanostruct 43:1266–1271

Ahmad N, Fazal H, Abbasi BH, Rashid M, Mahmood T, Fatima N (2010) Efficient regeneration and antioxidant potential in regenerated tissues of *Piper nigrum* L. Plant Cell Tissue Organ Cult 102:129–134

Ahmad A, Hadi F, Ali N, Jan AU (2016) Enhanced phytoremediation of cadmium polluted water through two aquatic plants Veronica anagallis-aquatica and *Epilobium laxum*. Environ Sci Pollut Res 23:17715–17729

Al-Dhabi N, Valan AM (2018) Environmentally-friendly green approach for the production of zinc oxide nanoparticles and their anti-fungal, ovicidal, and larvicidal properties. Nanomaterials 8:500

Ali N, Hadi F (2015) Phytoremediation of cadmium improved with the high production of endogenous phenolics and free proline contents in *Parthenium hysterophorus* plant treated exogenously with plant growth regulator and chelating agent. Environ Sci Pollut Res 22: 13305–13318

Ali N, Hadi F, Ali M (2019) Growth stage and molybdenum treatment affect cadmium accumulation, antioxidant defence and chlorophyll contents in *Cannabis sativa* plant. Chemosphere 236:124360

Allen SE, Grimshaw HM, Parkinson JA, Quarmby C (1974) Chemical analysis of ecological materials. Blackwell Scientific Publications

Andra SS, Datta R, Sarkar, Makris KC, Mullens CP, Sahi SV, Bach SB (2009) Induction of lead-binding phytochelatins in vetiver grass [*Vetiveria zizanioides* L.]. J Environ Qual 38:868–877

Anjum S, Abbasi BH (2016) Thidiazuron-enhanced biosynthesis and antimicrobial efficacy of silver nanoparticles via improving phytochemical reducing potential in callus culture of *Linum usitatissimum* L. Int J Nanomedicine 11:715–728

Astaneh RK, Bolandnazar S, Nahandi FZ, Oustan S (2018) Effect of selenium application on phenylalanine ammonia-lyase (PAL) activity, phenol leakage and total phenolic content in garlic (*Allium sativum* L.) under NaCl stress. Inf Process Agric 5:339–344

Ayaz M, Junaid M, Ullah F, Sadiq A, Subhan F, Khan MA, Ahmad W, Ali G, Imran M, Ahmad S (2016) Molecularly characterized solvent extracts and saponins from *Polygonum hydropiper* L. show high

anti-angiogenic, anti-tumor, brine shrimp, and fibroblast NIH/3T3 cell line cytotoxicity. Front Pharmacol 7:4

Azizullah A, Jamil M, Richter P, Häder DP (2014) Fast bioassessment of wastewater and surface water quality using freshwater flagellate *Euglena gracilis*—a case study from Pakistan. J Appl Phycol 26: 421–431

Balseiro-Romero M, Gkorezis P, Kidd PS, Van HJ, Weyens N, Monterroso C, Vangronsveld J (2017) Use of plant growth promoting bacterial strains to improve Cytisus striatus and Lupinus luteus development for potential application in phytoremediation. Sci Total Environ 581:676–688

Bates LS, Waldren RP, Teare I (1973) Rapid determination of free proline for water-stress studies. J Plant Soil 39:205–207

Bhattacharjee S (2016) DLS and zeta potential–what they are and what they are not? J Control Release 235:337–351

Cardwell A, Hawker D, Greenway M (2002) Metal accumulation in aquatic macrophytes from southeast Queensland, Australia. Chemosphere 48:653–663

Chang CC, Yang MH, Wen HM, Chern JC (2002) Estimation of total flavonoid content in propolis by two complementary colorimetric methods. J Food Drug Anal 10:178–182

Choudhary M, Jetley UK, Khan MA, Zutshi S, Fatma T (2007) Effect of heavy metal stress on proline, malondialdehyde, and superoxide dismutase activity in the *cyanobacterium Spirulina platensis*-S5. Ecotox Environ Safe 66:204–209

Choudhury S, Panda P, Sahoo L, Panda SK (2013) Reactive oxygen species signaling in plants under abiotic stress. Plant Signal Behav 8:23681

Chu TH (2014) Study on the growth and tolerance ability of *Polygonum hydropiper* L. and *Hymenachne acutigluma* (Steud.) Gilliland on Pb and Cd polluted soil. J Viet Environ 6:298–302

Cox A, Venkatachalam P, Sahi S, Sharma N (2016) Silver and titanium dioxide nanoparticle toxicity in plants: a review of current research. Plant Physiol Biochem 107:147–163

Dogaroglu Z, Koleli N (2017) Effects of TiO2 and ZnO nanoparticles on germination and antioxidant system of wheat (*Triticum aestivum* L.). Appl Ecol Environ Res 15:1499–1510

Duarte B, Caetano M, Almeida PR, Vale C, Caçador I (2010) Accumulation and biological cycling of heavy metal in four salt marsh species, from Tagus estuary (Portugal). Environ Pollut 158: 1661–1668

Ekmekçi Y, Tanyolaç D, Ayhan B (2009) A crop tolerating oxidative stress induced by excess lead: maize. Acta Physiol Plant 31:319–330

Elmer W, De LTR, Pagano L, Majumdar S, Zuverza-Mena N, Dimkpa C, Gardea-Torresdey J, White JC (2018) Effect of metalloid and metal oxide nanoparticles on Fusarium wilt of watermelon. Plant Dis 102: 1394–1401

Emad J, Ibrahem MK, Thalij KM, Amin S, Saleh B (2017) Biosynthesis of Zinc oxide nanoparticles and assay of antibacterial activity. Am J Biochem Biotechnol 13:63–69

Faizan M, Faraz A, Yusuf M, Khan ST, Hayat S (2018) Zinc oxide nanoparticles-mediated changes in photosynthetic efficiency and antioxidant system of tomato plants. Photosynthetica 56:678–686

Falkowska M, Pietryczuk A, Piotrowska A, Bajguz A, Grygoruk A, Czerpak R (2011) The effect of gibberellic acid (GA3) on growth, metal biosorption and metabolism of the green algae *Chlorella vulgaris* (Chlorophyceae) Beijerinck exposed to cadmium and lead stress. Pol J Environ Stud 20:53–59

Gao YY, Zhou QX (2013) Application of nanoscale zero valent iron combined with Impatiens balsamina to remediation of e-waste contaminated soils. Adv Mater Res 790:73–76

Garcia-Lopez JI, Zavala-García F, Olivares-Sáenz E et al (2018) Zinc oxide nanoparticles boosts phenolic compounds and antioxidant activity of *Capsicum annuum* L. during germination. Agronomy 8: 215.

Giannopolitis CN, Ries SK (1977) Superoxide dismutases: I. Occurrence in higher plants. Plant Physiol 59:309–314

Gong X, Huang D, Liu Y, Zeng G, Wang R, Wan J, Zhang C, Cheng M, Qin X, Xue W (2017) Stabilized nanoscale zerovalent iron mediated cadmium accumulation and oxidative damage of Boehmeria nivea (L.) Gaudich cultivated in cadmium contaminated sediments. Environ Sci Technol 51:11308–11316

Gong X, Huang D, Liu Y, Zeng G, Wang R, Xu P, Zhang C, Cheng M, Xue W, Chen S (2019) Roles of multiwall carbon nanotubes in phytoremediation: cadmium uptake and oxidative burst in *Boehmeria nivea* (L.) Gaudich. Environ Sci Nano 6:851–862

Gul I, Manzoor M, Hashim N, Kallerhoff J, Arshad M (2018) Comparison of EDTA, citric acid and TiO 2 nanoparticles to support Cd phytoaccumulation in spiked soil. Proceed. 2nd Int. Conf. Rec. Trends Environ Sci Eng 119.

Gunathilakae N, Yapa N, Hettiarachchi R (2018) Effect of arbuscular mycorrhizal fungi on the cadmium phytoremediation potential of *Eichhornia crassipes* (Mart.) Solms. Groundw Sustain Dev 7:477–482

Hadi F, Bano A, Fuller MP (2010) The improved phytoextraction of lead (Pb) and the growth of maize (*Zea mays* L.): the role of plant growth regulators (GA3 and IAA) and EDTA alone and in combinations. Chemosphere 80:457–462

Hadi F, Ali N, Fuller MP (2016) Molybdenum (Mo) increases endogenous phenolics, proline and photosynthetic pigments and the phytoremediation potential of the industrially important plant *Ricinus communis* L. for removal of cadmium from contaminated soil. Environ Sci Pollut Res 23:20408–20430

Hajra A, Mondal NK (2017) Effects of ZnO and TiO 2 nanoparticles on germination, biochemical and morphoanatomical attributes of *Cicer arietinum* L. Energ Ecol Environ 2:277–288

Hasan S, Talat M, Rai S (2007) Sorption of cadmium and zinc from aqueous solutions by water hyacinth (*Eichchornia crassipes*). Bioresour Technol 98:918–928

Hayat S, Hayat Q, Alyemeni MN, Wani AS, Pichtel J, Ahmad A (2012) Role of proline under changing environments: a review. Plant Signal Behav 7:1456–1466

Hoagland DR, Arnon DI (1950) The water culture method for growing plants without soil. Calif Agric Exp Stn Circ 347:31–32

Holm L, Doll J, Holm E, Pancho JV, Herberger JP (1997) World weeds: natural histories and distribution. John Wiley & Sons Inc, New York

Hua M, Zhang S, Pan B, Zhang W, Lv L, Zhang Q (2012) Heavy metal removal from water/waste water by nanosized metal oxides: a review. J Hazard Mater 211:317–331

Huang D, Qin X, Peng Z, Liu Y, Gong X, Zeng G, Huang C, Cheng M, Xue W, Wang X, Hu Z (2018) Nanoscale zero-valent iron assisted phytoremediation of Pb in sediment: impacts on metal accumulation and antioxidative system of Lolium perenne. Ecotoxicol Environ Saf 153:229–237

Huq A, Jamal JA, Stanslas J (2014) Ethnobotanical, phytochemical, pharmacological, and toxicological aspects of *Persicaria hydropiper* L. Delarbre. Evid Based Complement Alternat Med 1-11. https://doi.org/10.1155/2014/782830

Hussein MM, Abou-Baker NH (2018) The contribution of nano-zinc to alleviate salinity stress on cotton plants. R Soc Open Sci 5:171809

Ibrahim MH, Chee KY, Zain M, Amalina NA (2017) Effect of cadmium and copper exposure on growth, secondary metabolites and antioxidant activity in the medicinal plant Sambung Nyawa (*Gynura procumbens* (Lour.) Merr). Molecules 22:16–23

Ilboudo O, Tapsoba I, Bonzi-Coulibaly YL, Gerbaux P (2012) Targeting structural motifs of flavonoid diglycosides using collision-induced dissociation experiments on flavonoid/Pb2+ complexes. Eur J Mass Spectr 18:465–473

Iranbakhsh A, Ardebili ZO, Ardebili NO, Ghoranneviss M, Safari N (2018) Cold plasma relieved toxicity signs of nano zinc oxide in

Capsicum annuum cayenne via modifying growth, differentiation and physiology. Acta Physiol Plant 40:154

Jabeen N, Maqbool Q, Bibi T, Nazar M et al (2017) Optimised synthesis of ZnO-nano-fertiliser through green chemistry: boosted growth dynamics of economically important *L. esculentum*. IET Nanotechnol 12:405–411

Jamdagni P, Khatri P, Rana JS (2018) Green synthesis of zinc oxide nanoparticles using flower extract of *Nyctanthes arbor-tristis* and their antifungal activity. J King Saud Univ Sci 30:168–175

Jiamjitrpanich W, Parkpian P, Polprasert C, Kosanlavit R (2013) Trinitrotoluene and its metabolites in shoots and roots of Panicum maximum in nano-phytoremediation. Int J Environ Sci Dev 4:7–10

Jiang L, Liu Y, Liu S, Zeng G, Hu X, Hu X, Guo Z, Tan X, Wang L, Wu Z (2017) Adsorption of estrogen contaminants by graphene nanomaterials under natural organic matter preloading: comparison to carbon nanotube, biochar, and activated carbon. Environ Sci Technol 51:6352–6359

Jyoti K, Baunthiyal M, Singh A (2016) Characterization of silver nanoparticles synthesized using *Urtica dioic*L. leaves and their synergistic effects with antibiotics. J Radiat Res Appl Sci 9:217–227

Kabir M, Iqbal MZ, Shafiq M (2009) Effects of lead on seedling growth of Thespesia populnea L. Plant Soil Environ:194–199

Kalpana VN, Kataru BAS, Sravania N, Vigneshwaria T, Panneerselvamb A, Rajeswaria VD (2018) Biosynthesis of zinc oxide nanoparticles using culture filtrates of *Aspergillus niger*: antimicrobial textiles and dye degradation studies. Open Nano 3:48–55

Kamaraj R, Ganesan P, Vasudevan S (2015) Removal of lead from aqueous solutions by electrocoagulation: isotherm, kinetics and thermodynamic studies. Int J Environ Sci Technol 12:683–692

Khalil AT, Ovais M, Ullah I, Ali M, Shinwari ZK, Malik MM (2017) Biosynthesis of iron oxide (Fe_2O_3) nanoparticles via aqueous extracts of *Sageretia thea* (Osbeck.) and their pharmacognostic properties. Green Chem Lett Rev 10:186–201

Khan T, Abbasi BH, Khan MA, Shinwari ZK (2016) Differential effects of thidiazuron on production of anticancer phenolic compounds in callus cultures of *Fagonia indica*. Appl Biochem Biotechnol 179: 46–58

Kosyk O, Khomenko I, Batsmanova L, Taran NY (2017) Phenylalanine ammonia-lyase activity and anthocyanin content in different varieties of lettuce under the cadmium influence. Ukr Biochem J 89:85–91

Lagrimini LM (1991) Wound-induced deposition of polyphenols in transgenic plants overexpressing peroxidase. Plant Physiol 96: 577–583

Lai C, Wang MM, Zeng GM, Liu YG, Huang DL, Zhang C, Wang RZ, Xu P, Cheng M, Huang C, Wu HP, Qin L (2016) Synthesis of surface molecular imprinted TiO2/graphene photocatalyst and its highly efficient photocatalytic degradation of target pollutant under visible light irradiation. Appl Surf Sci 390:368–376

Lajayer BA, Ghorbanpour M, Nikabadi S (2017) Heavy metals in contaminated environment: destiny of secondary metabolite biosynthesis, oxidative status and phytoextraction in medicinal plants. Ecotoxicol Environ Saf 145:377–390

Li M, Ahammed GJ, Li C, Bao X, Yu J, Huang C, Yin H, Zhou J (2016) Brassinosteroid ameliorates zinc oxide nanoparticles-induced oxidative stress by improving antioxidant potential and redox homeostasis in tomato seedling. Front Plant Sci 7:615

Liang SX, Jin Y, Liu W, Li X, Shen SG, Ding L (2017) Feasibility of Pb phytoextraction using nano-materials assisted ryegrass: results of a one-year field-scale experiment. J Environ Manag 190:170–175

Liu X, Wang F, Shi Z, Tong R, Shi X (2015) Bioavailability of Zn in ZnO nanoparticle-spiked soil and the implications to maize plants. J Nanopart Res 17:1–11

Lou Y, Zhao P, Wang D, Amombo E, Sun X, Wang H, Zhuge Y (2017) Germination, physiological responses and gene expression of tall fescue (*Festuca arundinacea* Schreb.) growing under Pb and Cd. PLoS One 12:169495

Ma X, Wang C (2010) Fullerene nanoparticles affect the fate and uptake of trichloroethylene in phytoremediation systems. Environ Eng Sci 27:989–992

Ma X, Wang Y, Gao M, Xu H, Li G (2010) A novel strategy to prepare ZnO/PbS heterostructured functional nanocomposite utilizing the surface adsorption property of ZnO nanosheets. Catal Today 158: 459–463

Ma C, White JC, Xing B, Dhankher OP (2015) Phytotoxicity and ecological safety of engineered nanomaterials. Int J Plant Environ 1:9–15

Mahajan P, Dhoke S, Khanna A (2011) Effect of nano-ZnO particle suspension on growth of mung (*Vigna radiata*) and gram (*Cicer arietinum*) seedlings using plant agar method. J Nanotechnol **7**: 696535

Malar S, Vikram SS, Favas PJ, Perumal V (2016) Lead heavy metal toxicity induced changes on growth and antioxidative enzymes level in water hyacinths [*Eichhornia crassipes* (Mart.)]. Bot Stud 55:54–65

Michalak A (2006) Phenolic compounds and their antioxidant activity in plants growing under heavy metal stress. Pol J Environ Stud 15: 523–530

Mittal AK, Bhaumik J, Kumar S, Banerjee UC (2014) Biosynthesis of silver nanoparticles: elucidation of prospective mechanism and therapeutic potential. J Colloid Interface Sci 415:39–47

Miyake C, Shinzaki Y, Nishioka M, Horiguchi S, Tomizawa KI (2006) Photoinactivation of ascorbate peroxidase in isolated tobacco chloroplasts: Galdieria partita APX maintains the electron flux through the water–water cycle in transplastomic tobacco plants. Plant Cell Physiol 47:200–210

Miyazawa M, Tamura N (2007) Inhibitory compound of tyrosinase activity from the sprout of *Polygonum hydropiper* L.(Benitade). Biol Pharm Bull 30:595–597

Modena MM, Rühle B, Burg TP, Wuttke S (2019) Nanoparticle characterization: what to measure? Adv Mater 31:1901556. https://doi.org/10.1002/adma.201901556

Na GN, Salt DE (2011) The role of sulfur assimilation and sulfur-containing compounds in trace element homeostasis in plants. Environ Exp Bot 72:18–25

Nayyar H, Gupta D (2006) Differential sensitivity of C3 and C4 plants to water deficit stress: association with oxidative stress and antioxidants. Environ Exp Bot 58:106–113

Offor SJ, Mbagwu HO, Orisakwe OE (2017) Lead induced hepato-renal damage in male albino rats and effects of activated charcoal. Front Pharmacol 8:107

Pal S, Mondal S, Maity J, Mukherjee R (2018) Synthesis and characterization of ZnO nanoparticles using *Moringa oleifera* leaf extract: investigation of photocatalytic and antibacterial activity. Int J Nanosci Nanotechnol 14:111–119

Pant PP, Tripathi A (2014) Impact of heavy metals on morphological and biochemical parameters of *Shorea robusta* plant. Ekológia 33:116–126

Pawlak-Sprada S, Arasimowicz-Jelonek M, Podgórska M, Deckert J (2011) Activation of phenylpropanoid pathway in legume plants exposed to heavy metals. Part I. Effects of cadmium and lead on phenylalanine ammonia-lyase gene expression, enzyme activity and lignin content. Acta Biochem Pol 58:211–216

Pooja A, Lamba HS, Pankaj S (2018) Pharmacological, phytochemical, Biological evaluation and future prospects of *Polygonum hydropiper*. World J Pharmaceut Res 7:539–551

Prakash MJ, Kalyanasundharam S (2015) Biosynthesis, characterization, free radical scavenging activity and antibacterial effect of plant-mediated zinc oxide nanoparticles using *Pithecellobium dulce* and *Lagenaria siceraria* leaf extract. World Sci News 12:100–117

Prasad T, Sudhakar P, Sreenivasulu Y et al (2012) Effect of nanoscale zinc oxide particles on the germination, growth and yield of peanut. J Plant Nutr 35:905–927

Preetha PS, Balakrishnan N (2017) A review of nano fertilizers and their use and functions in soil. Int J Curr Microbiol App Sci 6:3117–3133

Priyanka N, Venkatachalam P (2016) Biofabricated zinc oxide nanoparticles coated with phycomolecules as novel micronutrient catalysts for stimulating plant growth of cotton. Adv Nat Sci Nanosci Nanotechnol 7:045018

Pullagurala VLR, Adisa IO, Rawat S, Kim B, Barrios AC, Medina-Velo IA, Hernandez-Viezcas JA, Peralta-Videa JR, Gardea-Torresdey JL (2018) Finding the conditions for the beneficial use of ZnO nanoparticles towards plants: a review. Environ Pollut 241:1175–2118

Qin F, Liu G, Huang G, Dong T, Liao Y, Xu X (2018) Zinc application alleviates the adverse effects of lead stress more in female *Morus alba* than in males. Environ ExpBot 146:68–76

Raliya R, Tarafdar JC (2013) ZnO nanoparticle biosynthesis and its effect on phosphorous-mobilizing enzyme secretion and gum contents in Clusterbean (*Cyamopsis tetragonoloba* L.). Agric Res 2:48–57

Raliya R, Saharan V, Dimkpa C, Biswas P (2017) Nanofertilizer for precision and sustainable agriculture: current state and future perspectives. J Agric Food Chem 66:6487–6503

Rizwan M, Ali S, Hussain A, Ali Q, Shakoor MB, Rehman MZ, Farid M, Asma M (2017) Effect of zinc- lysine on growth, yield and cadmium uptake in wheat (*Triticum aestivum* L.) and health risk assessment. Chemosphere 187:35–42

Salehi R, Arami M, Mahmoodi NM, Bahrami H, Khorramfar S (2010) Novel biocompatible composite (chitosan–zinc oxide nanoparticle): preparation, characterization and dye adsorption properties. Colloids Surf B: Biointerfaces 80:86–93

Saxena R, Tomar RS, Kumar M (2016) Exploring nanobiotechnology to mitigate abiotic stress in crop plants. JPSR 8:974

Sharmila G, Thirumarimurugan M, Muthukumaran C (2019) Green synthesis of ZnO nanoparticles using *Tecoma castanifolia* leaf extract: characterization and evaluation of its antioxidant, bactericidal and anticancer activities. Microchem J 145:578–587

Sheetal K, Singh S, Anand A, Prasad SJ (2016) Heavy metal accumulation and effects on growth, biomass and physiological processes in mustard. Indian J Plant Physiol 21:219–223

Singh S, Srivastava PK, Gupta M, Mukherjee S (2012) Modeling mineral phase change chemistry of groundwater in a rural-urban fringe. Water Sci Technol 66:1502–1510

Singh VP, Srivastava PK, Prasad SMJ (2013) Nitric oxide alleviates arsenic-induced toxic effects in ridged Luffa seedlings. PPB 71: 155–163

Singh A, Singh N, Afzal S, Singh T, Hussain I (2018) Zinc oxide nanoparticles: a review of their biological synthesis, antimicrobial activity, uptake, translocation and biotransformation in plants. J Mater Sci 53:185–201

Smirnov O, Kosyan A, Kosyk OJSB (2012) The Cycocel effect on flavonoids content and phenylalanine ammonia-lyase (PAL) activity in buckwheat (*Fagopyrum esculentum* Moench.) plant. Studia Biol 6: 247–252

Solanki P, Laura JJ (2018) Effect of ZnO nanoparticles on seed germination and seedling growth in wheat (*Triticum aestivum*). J Pharmacogn Phytochem 7:2048–2052

Song G, Gao Y, Wu H, Hou W, Zhang C, Ma H (2012) Physiological effect of anatase TiO2 nanoparticles on Lemna minor. Environ Toxicol Chem 31:2147–2152

Sthanadar IA, Sthanada AA, Yousaf M, Muhammad A, Zahid M (2013) Bioaccumulation profile of heavy metals in the gills tissue of Wallago attu (MULLEY) from Kalpani River Mardan, Khyber Pakhtunkhwa Pakistan. IJB 3:165–174

Sumanta N, Haque CI, Nishika J, Suprakash R (2014) Spectrophotometric analysis of chlorophylls and carotenoids from commonly grown fern species by using various extracting solvents. Res J Chem Sci 4:63–69

Tang WW, Zeng GM, Gong JL, Liang J, Xu P, Zhang C, Huang BB (2014) Impact of humic/fulvic acid on the removal of heavy metals from aqueous solutions using nanomaterials: a review. Sci Total Environ 468:1014–1027

Tang Y, Tian J, Li S, Xue C, Xue Z, Yin D, Yu S (2015) Combined effects of graphene oxide and Cd on the photosynthetic capacity and survival of Microcystis aeruginosa. Sci Total Environ 532:154–161

Tarafdar J, Raliya R, Mahawar H, Rathore IJAR (2014) Development of zinc nanofertilizer to enhance crop production in pearl millet (*Pennisetum americanum*). Agric Res 3:257–262

Tassi E, Pouget J, Petruzzelli G, Barbafieri M (2008) The effects of exogenous plant growth regulators in the phytoextraction of heavy metals. Chemosphere 71:66–73

Thema FT, Manikandan E, Gurib-Fakim A, Maaza M (2016) Single phase Bunsenite NiO nanoparticles green synthesis by *Agathosma betulina* natural extract. J Alloys Compd 657:655–661

Ullah S, Hadi F, Ali N, Khan S (2018) Foliar application of iron (Fe) improved the antioxidant defense and Cd accumulation potential of *Ricinus communis* under hydroponic condition. Water Air Soil Pollut 229:284

Ullah R, Hadi F, Ahmad S, Jan AU, Rongliang Q (2019) Phytoremediation of lead and chromium contaminated soil improves with the endogenous phenolics and proline production in Parthenium, Cannabis, Euphorbia, and Rumex species. Water Air Soil Pollut 230:40

Umar H, Kavaz D, Rizaner N (2019) Biosynthesis of zinc oxide nanoparticles using *Albizia lebbeck* stem bark, and evaluation of its antimicrobial, antioxidant, and cytotoxic activities on human breast cancer cell lines. Int J Nanomedicine 14:87–100

Velioglu Y, Mazza G, Gao L, Oomah B (1998) Antioxidant activity and total phenolics in selected fruits, vegetables, and grain products. J Agric Food Chem 46:4113–4117

Venkatachalam P, Jayaraj M, Manikandan R, Geetha N, Rene ER, Sharma N, Sahi S (2017a) Zinc oxide nanoparticles (ZnONPs) alleviate heavy metal-induced toxicity in *Leucaena leucocephala* seedlings: a physiochemical analysis. Plant Physiol Biochem 110:59–69

Venkatachalam P, Priyanka N, Manikandan K, Ganeshbabu I, Indiraarulselvi P, Geetha N, Muralikrishna K, Bhattacharya R, Tiwari M, Sharma NJPP (2017b) Enhanced plant growth promoting role ofphycomolecules coated zinc oxide nanoparticles with P supplementation in cotton (*Gossypium hirsutum* L.). Plant Physiol Biochem 110:118–127

Vimala K, Sundarraj S, Paulpandi M, Vengatesan S, Kannan S (2014) Green synthesized doxorubicin loaded zinc oxide nanoparticles regulates the Bax and Bcl-2 expression in breast and colon carcinoma. Process Biochem 49:160–172. https://doi.org/10.1016/j.procbio.2013.10.007

Wang X, Cai W, Lin Y, Wang G, Liang C (2010) Mass production of micro/nanostructured porous ZnO plates and their strong structurally enhanced and selective adsorption performance for environmental remediation. J Mater Chem 20:8582–8590

Wang P, Zhang S, Wang C, Lu JJE (2012) Effects of Pb on the oxidative stress and antioxidant response in a Pb bioaccumulator plant *Vallisneria natans*. Ecotoxicol Environ Saf 78:28–34

Wang J, Ye S, Xue S, Hartley W, Wu H, Shi L (2018) The physiological response of *Mirabilis jalapa* Linn. to lead stress and accumulation. Int Biodeterior Biodegradation 128:11–14

Yang F, Liu C, Gao F, Su M, Wu X, Zheng L, Hong F, Yang P (2007) The improvement of spinach growth by nano-anatase TiO 2 treatment is related to nitrogen photoreduction. Biol Trace Elem Res 119:77–88

Yang Q-w, H-m K, S-j L, Zeng Q (2018) Phytoremediation of Mn-contaminated paddy soil by two hyperaccumulators (*Phytolacca*

americana and *Polygonum hydropiper*) aided with citric acid. Environ Sci Pollut Res 25:25933–25941

Yedurkar S, Maurya C, Mahanwar P (2016) Biosynthesis of zinc oxide nanoparticles using *Ixora coccinea* leaf extract A green approach. Open J Synth Theory Appl 5:1–14

Zafar H, Ali A, Ali JS, Haq IU, Zia MJ (2016) Effect of ZnO nanoparticles on *Brassica nigra* seedlings and stem explants: growth dynamics and antioxidative response. Front Plant Sci 7:535

Zahir A, Abbasi BH, Adil M, Anjum S, Zia M (2014) Synergistic effects of drought stress and photoperiods on phenology and secondary metabolism of *Silybum marianum*. Appl Biochem Biotechnol 174: 693–707

Zhao L, Hernandez-Viezcas JA, Peralta-Videa JR, Bandyopadhyay S, Peng B, Munoz B, Keller AA, Gardea-Torresdey JL (2013) ZnO nanoparticle fate in soil and zinc bioaccumulation in corn plants (*Zea mays*) influenced by alginate. Environ Sci-Proc Imp 15:260–266